Laser beam interactions with metal matrix AlSi alloy/SiCp composites

A. Grabowski [a,*], M. Nowak [a], J. Śleziona [b]

[a] Institute of Physics, Silesian University of Technology,
ul. Krasińskiego 8, 40-019 Katowice, Poland

[b] Faculty of Materials Science and Metallurgy, Silesian University of Technology,
ul. Krasińskiego 8, 40-019 Katowice, Poland

* Corresponding author: andrzej.grabowski@polsl.pl

Materials

ABSTRACT

Purpose: The purpose of the research discussed in this paper was to identify the physical processes that take place when a focused laser beam acts on a metal matrix composites reinforced with silicon carbide particles (AlSi alloy/SiCp).

Design/methodology/approach: Based on theoretical models, an analysis was carried out of the interaction between a focused laser beam and the individual components of an AlSi alloy/SiCp composite material: the reinforcement particles, SiC, and the AlSi-alloy metal matrix. Assuming effective parameters of the composite material, the energy necessary to melt a unit thickness of the composite was determined according to basic principles.

Findings: It has been shown that the time during which the melting point of the composites' individual components is achieved varies. Modelling based on the energy and mass conservation law provides for the necessary laser beam energy to melt a unit thickness of a composite.

Research limitations/implications: In the case of cutting of a composite, however, some effects connected with the thermal field fluctuation occur, which are not explained in the model. A striated structure appears on the composite edges cut with a laser.

Practical implications: The research results enable optimization of laser machining parameters, such as laser radiation intensity or the laser beam operation time. This allows reducing the thermal overload that appears in the case of too high density of the laser energy.

Originality/value: Application of thermophysical and optical parameters of composite's individual components yields more information about the processes that take place when scanning the metal matrix composite surface with a high intensity laser beam.

Keywords: Metal matrix composites; Heat treatment; Laser modelling; Laser treatment

1. Introduction

Aluminium matrix composites reinforced with silicon carbide particles belong to a group of modern engineering materials. Due to their mechanical, thermal and electrical properties, they are widely applied in the automotive and aircraft industries [17] as well as in electrical engineering and microelectronics. These composites are more and more frequently applied for manufacturing commonly used objects and sports equipment.

Application of composite materials in an industrial scale depends, to a large degree, on effective capacity for their machining at both the premachining level and at the finishing level [5, 15]. The presence of hard ceramic particles in composite materials makes them difficult to machine. Currently, the most effective methods of composite materials' machining are based on

the use of diamond tools [14]. Among non-traditional methods, there are electroerosion treatment or cutting by means of a focused stream of water or air. Other non-traditional methods include laser techniques based on a focused laser beam of high intensity as a „no-contact tool" used for machining of materials. The laser methods are successfully applied in the industry for machining of metals and their alloys, semi-conductors, ceramic materials and plastic materials [6, 12, 13, 16]

The purpose of this article is to analyze the mechanisms of the laser energy radiation coupling into aluminium matrix composites reinforced with silicon carbide particles (AlSi-alloy/SiC_p) – the heterogeneous structural material consisting two different components. In this paper the experimental results of the optical reflectance properties of AlSi-alloy/SiC_p were presented and discussed. Next the experimental data were used in mathematical models to estimate laser melt and cut depth of the AlSi-alloy/SiC_p. Based on model, the relationship between the cutting speed and the laser power for good quality cuts of AlSi-alloy/SiCp is presented. Also the formation of striations has received much attention because that they strongly affect the quality of laser cutting of the AlSi-alloy/SiC_p. The microstructure of the heat affected zone at the kerfs was studied with a scanning electron microscope. The XRD results about the crystalline phase's of the laser beam cutting kerfs of the AlSi-alloy/SiC_p composite are reported.

2. Physical formulation of the laser beam interaction with AlSi-alloy/SiCp

During laser machining, the energetic efficiency in transferring energy from a focused laser beam to a material depends first of all on the optical and thermal properties of the machined material. Other factors which also determine the laser machining effectiveness are the so-called laser beam parameters, including: the laser beam radiation intensity, the beam energy distribution and the operation time. The electromagnetic radiation of a laser beam emitted from the modern industrial high-power lasers can be focused through the laser head's optical system to sizes comparable to the laser's electromagnetic radiation wavelength. In the case of CO_2 lasers of wavelength λ = 10.6μm, the beam diameters are in the order of hundred's micrometers.

In Fig. 1a typical structure of AlSi-alloy/SiC_p composite material, reinforced with SiC_p ceramic particles, obtained by casting process [18] is shown. It can be seen that the main phases of this AlSi-alloy matrix material are: primary α-Al dendrites (white), and eutectic mixture of Si and α-Al phase. The SiC particles are the polycrystalline silicon carbide (mostly β-SiC type). It is shown in Fig. 1a that there is a spread size distribution for SiC_p particles, which characteristically vary for different regions in the metal matrix. Moreover, some primary Si single crystals, as well as the voids (pores) were also observed in the investigated specimens. These pores were mostly associated with the SiC_p particles and located at the interface between SiC_p particles and AlSi-alloy (Fig. 1b). Also the particles clusters were the place into the AlSi-alloy/SiC_p where the pores are observed most frequently [7].
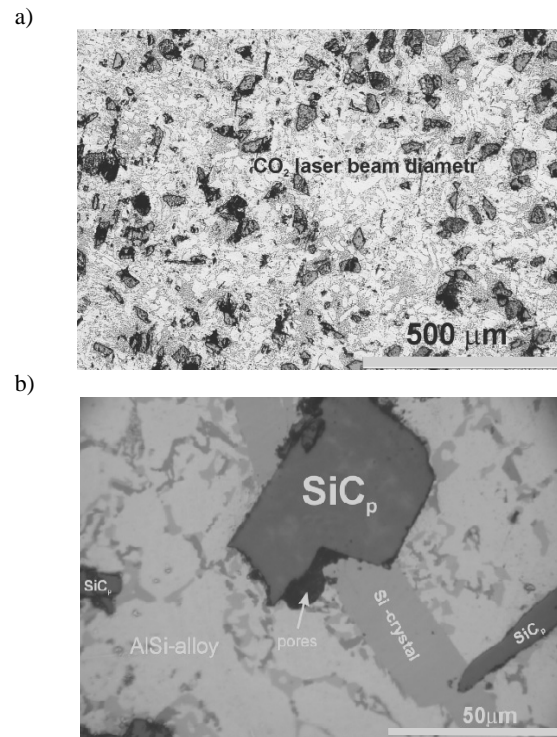

Fig. 1. Optical micrographs of an AlSi-alloy metal matrix with the distribution of the vol. 15% SiCp particles (dark), obtained by casting method (a), The interfacial region of the AlSi-alloy matrix and SiCp particle (b)

When comparing the SiC_p particles sizes and their arrangement in the AlSi-alloy matrix in relation to the size of a focused beam of the CO_2 laser (Fig. 1), it should be affirmed that the laser beam during scanning of the composite surface reacts alternately with the metallic matrix of the AlSi-alloy and the SiC_p reinforcement particles. In such cases, instead of using the averaged (effective) physical properties of a composite material, the individual physical properties of each of its components should be taken into consideration.

Fig. 2 shows the changes in normal optical reflectance measured along the laser cutting line for AlSi-alloy/SiC_p composite surface presented in Fig. 1. It is evident that during the laser beam scanning there is a change of around 15% in the amplitude of the optical reflectance, hence the local value of the absorptivity of laser radiation changes.

From the physical point of view the main components of AlSi alloy/SiCp composite material: the SiCp particles and AlSi alloy metal matrix have different absorption values of electromagnetic laser radiation [20].

The energies of photons emitted by CO_2 and Nd:YAG lasers as well as by a high-power diode laser (HPDL) are much lower than the energy of the optical break for silicon carbide, which for a material of the β-SiC type amounts $E_g \approx 3.2eV$. In the case of laser beam photons acting on SiC, there will be no highly-efficient, in terms of energy, interband absorption of photons in the material. Absorption in SiC of high-intensity laser radiation ($I_o > 1kW/cm^2$) of photons' energy $hv < Eg$ will take place mostly

via „multiphoton interband transition". Such absorption will cause thermal generation of free charge carriers in SiC, which carriers will next induce additional absorption of laser radiation.
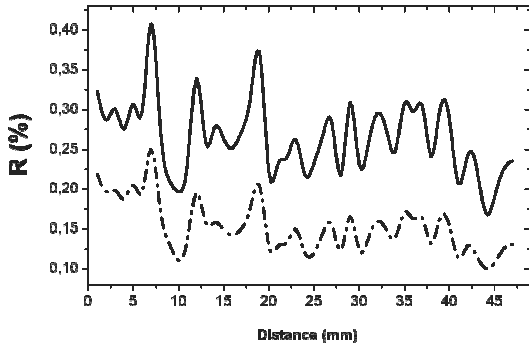

Fig. 2. Normal optical reflectance as a function of distance along the laser cutting line of AlSi alloy/SiCp 15 vol. % composite work piece before laser cutting, for two wavelengths electromagnetic radiations (solid line: $\lambda = 1.06\mu m$, dashed line: $\lambda = 0.5\mu m$)

Where a metallic matrix is present (AlSi-alloy), the laser beam photons' energy is absorbed by free carriers in the conduction band. As a result of the photon/electrons interaction, the excited electrons have kinetic energy which, as a result of the electron/photon interaction, is next transferred to the crystal lattice, thus causing an increase in its inner energy. It needs emphasizing that the laser radiation absorption processes and their speed differ in those two principal components of the composite, which translates into the speed of the laser beam energy transition to their inner energy.

Electromagnetic radiation of a laser beam is absorbed in the surface layer of a material, its depth being an inverse of the material's absorptivity, $1/\alpha(\lambda)$. The absorption depth values determined for CO_2 laser radiation ($\lambda = 10.6\mu m$), are $1/\alpha_{SiC} = 0.68mm$ for SiC and $1/\alpha_{SiC} = 0.03mm$ for the AlSi alloy. This means that in the first phase of its operation, the laser beam energy is emitted in a thin close-to-surface layer of the material, of thickness much smaller than the size of the focused laser beam. In such case, using the thermal conductivity equation for one dimension and assuming that no phase transition is taking place, it is possible to estimate, based on equation (1), the temperature $T(t)$ changes of SiC and AlSi surfaces in time [1].

$$T(t) - T_0 = \frac{I_0 A}{K\alpha}\left[2\alpha\sqrt{\frac{at}{\pi}} + \exp(\alpha^2 at)erfc(\alpha\sqrt{at}) - 1\right] \quad (1)$$

where:
T_0 – is the ambient temperature,
I_o – the laser power density at the material surface (W/m²),
α – the absorption coefficient (1/m),
A – absorption of the component at perpendicular incidence,
K – the thermal conductivity,
a – thermal diffusivity ($a=K/c_p\rho$),
c_p – specific heat,
ρ – mass density,
t – the time of laser interaction with the component.

For the calculations with equation (1), the average temperature independent thermophysical constants of the conductivity, density and specific heat values for SiC_p and for AlSi-alloy components are used.

Obtained from equation 1, the time evolution of the surface temperature variation rate for AlSi-alloy and SiC materials were plotted in Fig. 3.
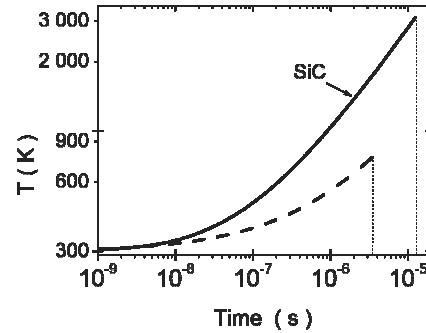

Fig. 3. Time dependence of the surface temperature in SiC (solid line) and AlSi-alloy (dashed line) irradiated by a CO_2 laser beam of laser radiation intensity $I_o = 10^7$ (W/cm²), plotted from equation (1)

In Fig. 3 it could be seen the exponential growth of the surfaces temperature for both components at a longs time of laser beam interaction. The melting temperature $T_m = 850K$ for AlSi-alloy material could be reached after 5 μs time whereas for SiC_p particle the sublimation temperature $T_m = 3103$ K, after $t = 12$ μs. During that short time as the surfaces reached the melting temperature the laser energy is converted to heat and next started to diffuse into the deep of material. The calculated diffusion lengths $\delta = 2\sqrt{\kappa_{av}t}$ of the heat are equal $\delta_{AlSi-alloy} = 32\mu m$ and $\delta_{SiC} = 58\mu m$, these values are large than appropriate absorption depth of the CO_2 laser radiation.

These results indicate that the melting time of the AlSi-alloy metal matrix is almost two times shorter than for SiC_p particle at the same laser radiation intensity.

When a laser beam is irradiated on AlSi-alloy/SiC_p material surface, a portion of laser energy is absorbed and next conducted into the interior of the material. If the absorbed energy is high enough, material surface will melt and the melting front will propagate into the work piece. Boiling and vaporization can also occur at the free surface of the melt. For AlSi-alloy/SiC_p the melting heat of the components is much smaller than their evaporation heat. Therefore, a more economical method, which does not require high laser power, is gas-assisted laser cutting, in which the composite material is locally (within the spot of focused laser radiation) heated to the melting point (particularly the low-melting AlSi-alloy matrix) and next is entrained due to intense blowing of the assisted gas jet [12].

In order to determine the laser beam energy necessary to melt a unit thickness of the composite material, a theoretical model was utilized in the study, based on the energy conservation law and the mass flux continuity principle.

The overall energy and mass balance equations in accordance with the geometry of laser cutting setup presented in Fig. 4, for the laser beam radiation takes the form [9]:

$$E_a = E_p + E_c + E_{loss} \qquad (2)$$

where:
E_a – laser beam energy absorbed by the AlSi-alloy/SiC$_p$ material,
E_p – the energy involved in the heating, boiling and the phase change,
E_c –energy lost due to heat conduction from the melted to the surround solid region AlSi-alloy/SiC$_p$. for conduction.

$$v_b w_m d_m = (v_m + v_b)(w_m - w_k)d_m + f_w w_m d_m \qquad (3)$$

where:
v_b – the laser beam scanning velocity,
v_m – the average velocity of liquid composite material in the kerf,
f_w – a fraction of the total amount of composite material melted by the laser beam,
w_k – the kerf width (close to the laser beam diameter),
$w_m - w_k$ – the difference is equal the thickness of thermal layer close to heat affected zone (HAZ) size.
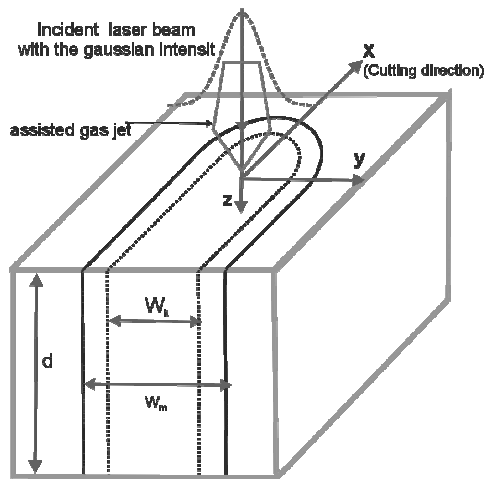

Fig. 4. Geometry of laser cutting model used in this study

3. Experiments

AlSi-alloy/SiC$_p$ composite (Table 1) used in this study was fabricated using metallurgy technique (liquid-phase processes). Processing of the AlSi-alloy/SiC$_p$ composite consist of mixing pre-heated SiC particulates and liquid aluminium alloy, melt stirring and ingot cast [18]. The metal matrix was commercial aluminium alloy (in wt %: Si – 12, Cu – 1.1, Mg – 0.5, Ni – 0.95). The reinforcement particulates are high purity silicon carbide (β-SiC) with an average diameter of 50μm. The plate of AlSi-alloy/SiC$_p$ samples material with dimension 150mm by 80mm and thickness from 3 to 15mm were used in experiment. The surfaces of AlSi-alloy/SiC$_p$ samples were prepared with 600 grit SiC paper for all optical and laser cutting experiments.

Table 1.
Typical values of the physical properties of AlSi alloy/SiC$_p$ composites material and their components used in the current set of predictions

Physical properties	Units	Values of physical properties		
		AlSi-alloy	SiC$_p$ (β)	AlSi-alloy/ SiC$_p$ 15 vol. %
ρ (300 K)	kg·m^{-3}	2650	3210	2838
T_m	K	850	2980	823
c_p (300 K)	J·kg^{-1}·K	913	690	896
k (300 K)	W·m^{-1}·K^{-1}	136.2	244	97.9
L_m	kJ·kg^{-1}	390	Si	324
L_b	kJ·kg^{-1}	10.7·10^3	Si	10.7·10^3
A (10.6μm)	–	0.06	0.25	0.17

Laser cutting experiments were performed using CO_2 lasers: TLF4000 (Trumpf), operating in pulsed mode and a continuous Spectra-Physics 820. A beam delivery system with 127mm ZnSe lens was used. The diameter of the focused laser beam was 0.25mm and the focus position was the upper surface of the AlSi-alloy/SiC$_p$ samples. The laser cutting was performed with assist inert gas (nitrogen) at gas pressures ranging from 10-16 bar. The coaxial assist gas used for cutting was delivered to the cut point via copper cutting nozzle. The parameters of the cutting nozzle were: nozzle orifice size ϕ=1.5mm, the stand off distance (0.8-1.2) mm.

The shape of the laser cutting kerfs and the microstructural characterization studies of the cut edge were conducted on the AlSi-alloy/SiC$_p$ in order to investigate the morphology of the HAZ region and to evaluate the distribution of the SiC particles. These studies were carried out primarily using a optical microscope (Olympus GX71) and next scanning electron microscope (Hitachi-S3400N). The geometrical characteristics of the surface roughness laser cut edge were measured with contact instruments Surtronic3+, Taylor-Hobson.

Fig. 5 presents the theoretical dependencies, calculated from equations 2 and 3, of the laser beam power falling to a unit thickness of a melted composite material (P/d) depending on the laser cutting speed V_b. The calculations were made for different laser radiation absorption values from the range of 0.17-0.3.

The obtained theoretical dependencies indicate a linear dependence between the P/d and V_b parameters for the investigated composite material. The presented results show that the laser radiation absorption value has a very strong influence on the course of the P/d vs. V_b dependence. An increase in absorption of 0.1 leads to a considerable decrease of the P/d quotient value, which is particularly visible at high laser beam speeds, V_b.

The experimental results obtained for laser cutting of the composite were put on the theoretical results presented in Fig. 5. The best compliance of the model was obtained for the assumed constant absorption value A = 0.2. This value should be considered effective for the whole investigated composite material. The observed compliance of the experiment with the theoretical model is particularly good for high speeds of the laser beam. The obtained theoretical results indicate a possibility of optimizing the laser machining parameters for the AlSi-SiC composite material.
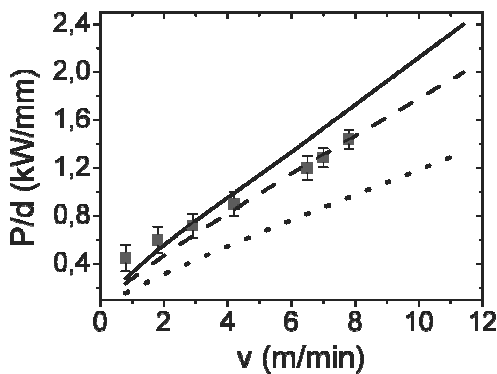
Fig. 5. Power of laser beam per unit depth of AlSi-alloy/SiC$_p$ 15 vol. % composite as a function of the cutting speed velocity calculated for three different absorptivity values (A = 0.17 – solid line, A = 0.2 – dashed line, A = 0.3 – dotted line; symbol ■ indicate the experimental results obtained for CO$_2$ laser cutting with nitrogen assist gas)

In case of prediction of the theoretical models as the SiC$_p$ particle volume increases in the AlSi-alloy/SiC$_p$ composite materials, the model predicts that the largest cutting thickness can be obtained. We can see it in Fig. 6. The model gives such prediction which is related to a slightly greater absorptivity value and the lower heat conductivity of the AlSi-alloy/SiC$_p$ composite in comparison to AlSi-alloy [10].
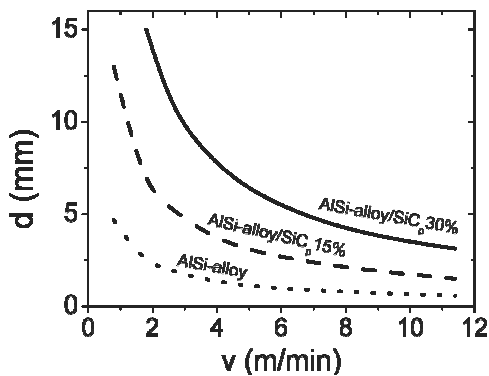

Fig. 6. Calculated cutting depth for AlSi-alloy/SiC$_p$ composites as a function of the cutting speed, for different volume fraction of SiC$_p$ particles and constant CO$_2$ laser beam power P = 4 kW

In the gas-assisted laser cutting technique laser machining parameters are also important as the optical and thermo-physical properties of material. The are first of all the average laser beam power and next:
- frequency and duty cycle,
- velocity of the cutting process,
- the nozzle shape as well as the pressure of the assisted gas,
- distance from bottom of nozzle tip to the top of the material (stand-off distance),
- the focal position of the laser beam.

For the experimental verification of the influence of the machining parameters on the laser cut quality, the cuttings have been carried out under the same parameters laser cutting for AlSi-alloy/SiC$_p$ composite as well as for AlSi-alloy metal matrix comparative work piece. The measured surface roughness R$_a$ (root-mean-square average) of the middle part of the AlSi-alloy/SiC$_p$ 15 vol. % cut surfaces was R$_a$ = (17,1 ±3,4) μm, and for AlSi-alloy the R$_a$ = (2,9 ±0,8) μm. It is evident to laser cutting that the presence of 15 vol. % SiC$_p$ particles changes the dynamic of the cutting front, consequently the R$_a$ increase.

Obviously the surface roughness is strongly related to striation frequency [4]. The microstructure of the cut kerf was studied with a scanning electron microscope (SEM) using secondary as well as backscattered electron for image generation. Fig. 7 shows a typical morphology of a laser cut kerf of the thick AlSi-alloy/SiC$_p$ composite materials with supersonic jet of nitrogen used as an assist gas [11]. In Fig. 7 the three distinct zones are seen. In Zone I the keyhole is initiated, the erosion front is created, and a very thin film of molten AlSi-alloy/SiC$_p$, continuously produced from the solid substrate, is constantly blown down (to Zone II) by the high pressure of the assist gas. There is no regular striations observed in this zone and the heat affected zone (HAZ) is no thicker than 40μm.
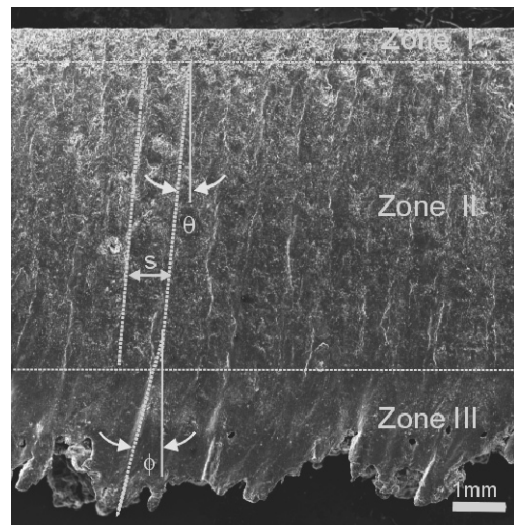

Fig. 7. SEM picture of the typical example of cut kerf 8mm thick AlSi-alloy/SiC$_p$ 15 vol. % composite specimen cutting with laser; cutting parameters: average power of CO$_2$ laser P = 4kW, pulse repetition rate f = 10kHz, cutting speed v = 1 (m/min), nitrogen jet assistance gas pressure 16 bar, standoff distance 2 mm, focal position the laser beam relative to top surface -6.5mm

In the Zone II the free flow of molten composite is transformed into a constricted flow and in a consequence, the melt film thickness becomes greater. In Zone II striations appear on the cut kerf as relatively regular straight lines which run at often slight angles Θ, to the laser beam axis. This angle depends on the laser parameters (e.g. the cutting speed), but for the better cutting of the 8mm thick AlSi-alloy/SiC$_p$ composite this angle was almost constant, equal $\Theta° \approx 5°$. The angle of striations could be identified

with the cutting front angle. At the angle of $\Theta^o \approx 5^o$ the maximum Fresnel absorption, occur for AlSi-alloy/SiC$_p$ and circular polarized CO_2 laser radiation [11]. It is interesting that similar striations image for AlSi-alloy/SiC$_p$ composite was observed for wide range of CO_2 laser pulse repetition rates (500-10 000) Hz at constant cutting speed velocity and laser beam power.

The average wavelength s of the periodic structure that appeared on the cut kerf in Zone II (Fig. 7) was experimentally determined as s = (0.77 ±0.02) mm. The s value is close to thickens of the molten layer (w_m–w_k), whereas s/Δt physically represents the rate of change of the molten layer in the interval time Δt and can be given approximately by the differences V_m-V_b.

By knowing the laser cutting speed (v_b = 1m/min) the temporal frequency of these cutting parameters was determined as a 22Hz. The striations frequency is a characteristic element of a given metallic material and laser parameters process; they are the spitting image of the superposition of successive melting isotherms generated by the laser beam. The striation frequency value observed for AlSi-alloy/SiC$_p$ composite could be low compared to the frequencies observed during cutting the aluminium alloy matrix as well as other metallic materials where frequencies are one order higher [19].

The zone III starts at the bottom kerf the AlSi-alloy/SiC$_p$ composite work piece. The striation transition from Zone II to III (Fig. 7) creates the „double slope”. The angles of straight lines change from $\Theta^o \approx 5^o$ to $\phi = 15°$. This phenomenon, observed also by Duan [8], can be explained by the significant change in melt film thickness in this part of kerf. Because of the high surface tension, the gas jet cannot remove completely all the melt so is covered in rapidly solidified melt (dross) along the bottom edge.

There have been numerous research efforts in order to understand the formation of striations on the kerf. Arata et al. and first of all Schuocker [4, 8, 19] suggested that the fluctuations in absorbed laser power can induce both temperature and molten layer thickness oscillations, thus causing striations to occur.

In the case of heterogeneous materials such as AlSi-alloy/SiC$_p$, the changes in the optical absorptivity are natural (Fig. 2). Consequently the dynamic changes in laser energy absorption by the AlSi-alloy/SiC$_p$ surface during laser scanning lead straight to the layer thickness oscillations.

The microstructural characteristic of laser cut edge in the cross sectioned view are shown in Fig. 8. Two zones with distinct microstructural features can be clearly observed in this figure. The laser alloyed zone and the heat affected one (HAZ). In the laser alloyed zone the significantly smaller size of the crystal of the AlSi-alloy matrix compared to non-treated material was observed. This effect was also observed in other laser material treatments [2]. As indicated in Fig. 8 the depth of above two zones could be easily measured under the microscope. The variation in depth along the kerfs eight millimetres thick AlSi-alloy/SiC$_p$ specimen determined is illustrated in Fig. 8.

The HAZ depths presented in Fig. 8 is correlated with the zones observed in Fig. 7. At the top part of the kerf, the SiC$_p$ particles were not melted during the laser cutting. The full size SiC$_p$ particles are close to the laser cutting surface. At the lower part of the AlSi-alloy/SiC$_p$ kerf, the extent of the HAZ increases. The maximum value of the HAZ was observed at the bottom kerf of the AlSi-alloy/SiC$_p$ composite materials. Interesting interpretation of the micro and macroscopic structure that could be used to characterize the observed HAZ Zones in AlSi-alloy/SiC$_p$ composite was described in work [2].
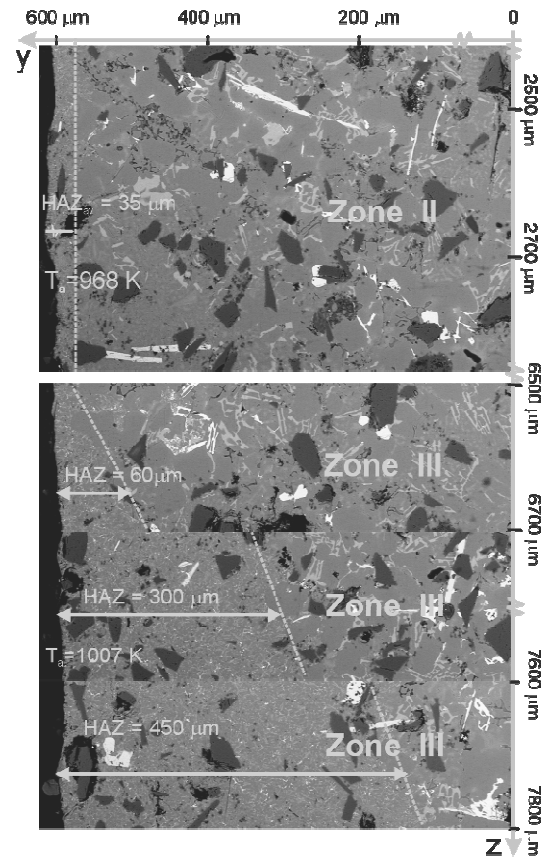

Fig. 8. Cross-section SEM micrograph of the HAZ depth in the 8mm thick of the AlSi-alloy/SiC$_p$ 15 vol. % composite specimen cutting with laser; cutting parameters: average power of CO_2 laser P = 4kW, pulse repetition rate f = 10kHz, nitrogen jet assistance gas pressure: 16 bar

It can be seen in Fig. 8 that the HAZ depth increases from 35μm to 450μm. The energy balance and the Stefan conditions at the solid-liquid interface can determine the characteristic temperature of the melt T_a [9]:

$$T_a = S_{HAZ} \frac{\rho L_m}{2K} v_b + S_{HAZ} \frac{T_m - T_o}{2(\kappa w_k)^{1/2}}(v_b)^{1/2} + T_m \qquad (4)$$

where:
S_{HAZ} – the average thickness of the recast layer in the kerf,
L_m – latent heat of melting.

The calculated temperature T_a in Zone I and II (Fig. 6) is almost constant and equals $T_a \approx 968K$. For Zone III the temperature Ta increases above 1000K. The increase in T_a calculated from equation 4 can be explained by the fact that the molten layer thickness S_{HAZ} becomes bigger in size in Zone III. Which occurs when molten composite move in the through-thickness direction of the composite (Z direction, Fig. 4), molten composite material accumulates at the bottom of the base material and subsequently is cooled.

To obtain information about the crystalline phase's composition and the elements distributions at the laser cut kerf of the AlSi-alloy/SiC$_p$ composites, the X-ray diffractometry (XRD) and X-ray energy dispersive spectroscopy (EDS/XR) analysis was undertaken. The obtained X-ray diffraction spectra for different parts of the laser cut kerf for wide range of laser beam energy density (up to P/vR$_b$ = 2.5x10^9, J/m^2) do not show that new phases to be formed in the AlSi-alloy/SiC$_p$ composite materials laser cut kerf. The some changes in X-ray diffraction spectra in comparison with not laser treated area were observed only for AlSi-alloy/SiC$_p$ material derived from middle part of the cutting grow. This part of material absorbed the most of laser energy and was melted and next blowing by the assisted gas outside the cut grove. The comparison of X-ray diffraction spectra's showed at Fig. 9 indicated that the diffraction amplitude peaks of crystalline phase SiC$_p$ are lower, what confirm that some polycrystalline SiC$_p$ particles decomposed.
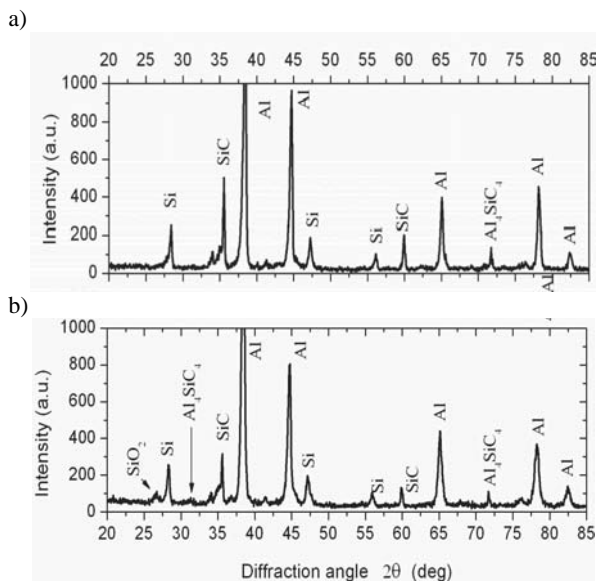

Fig. 9. X-ray diffraction spectra of AlSi alloy/SiC$_p$ 15 vol. % composites materials: after laser processing (a), untreated laser (b)

Decomposition of the SiC$_p$ particles is connected with the high heat input associated with laser cutting. In the kerf zone SiC particle melts and provides C for reaction with Al to form Al$_4$C$_3$ based on the reaction as follows [3, 21]:

$$4Al+3SiC \rightarrow Al_4C_3+3Si \qquad (5)$$

The absent of aluminium silicon carbides phases at the laser cut kerfs (Fig. 7) indicated that interfacial reaction did not take place during laser cutting [3]. This must be due to the short laser beam/composite material interaction time and second the high levels of silicon (AlSi-alloy are eutectic composition with 12.6 wt. % Si content) in the AlSi-alloy/SiC$_p$ composite, metal matrix reduce the tendency to form aluminium silicon carbides.

Fig. 9 shows that with additional phases only SiO$_2$ and Al$_4$SiC$_4$ was observed in AlSi-alloy/SiC$_p$ composites after processing with laser beam radiation 10^7 (W/cm^2).

4.Conclusions

A description of the interaction between a focused laser beam and a composite material is a complex issue since the shifting laser beam reacts alternately with the composite components, the latter being materials of different thermophysical and optical properties. The reason for this is a different degree and time of melting the composite components.

As the research has shown, for constant laser beam radiation intensity, the SiC$_p$ particles' melting time is almost twice longer than for the composite's metallic matrix. This implies the capacity for selecting such laser machining parameters that the laser beam would melt (damage) the SiC reinforcement particles in a composite to a small degree only. As a result, higher quality of the laser machined composite surfaces would be ensured. The properly selected laser radiation intensity induces lower thermal overload of the composite, which has a direct influence on the dynamics of the chemical reactions that take place in the heat affected zone of the laser machined composite. At too high laser beam energy, an Al$_4$C$_3$ compound is formed in that zone, which reduced the quality of the laser machined surfaces.

The applied theoretical model based on the principal laws of energy and mass conservation allows correct forecasting of the degree to which the composite material will melt when using a laser beam of predetermined power.

As results from the carried out experiments of laser cutting of composite materials, the observed instability of the composite's cutting front resulting from changes in the laser radiation absorption, translates into the observed roughness of composite kerfs.

Additional phenomena that occur during laser cutting of a composite material are the consequence of movement of the melted layer of the liquid composite in the kerf. The liquid layer of melted composite, formed on the front and edges of the kerf, is blown out by a nitrogen stream. The different values of the layer's thickness and its temperature induce changes in the viscosity coefficient as well as in the surface tension of the layer. In consequence, increased roughness of laser-cut composite's edges is observed.

Three distinct zones on the cut kerf have been identified. The zones of regular striations give information about the dynamic process of laser cutting and could be a method of characterize very difficult process of laser cutting composite material with assist gas. The formation of striations affect on the quality of laser cutting of composite.

Acknowledgements

References

[1] S.I. Ansimov, V.A. Khokhlov, Instabilities in Laser-Matter Interaction, CRC Press, Inc., Boca Raton, 1995.

[2] M. Cholewa, Simulation of solidification process for composite micro-region with incomplete wetting of reinforcing particle, Journal of Materials Processing Technology 164-165 (2005) 1181-1184.

[3] N.B. Dahotre, T.D. McCay, M.H. McCay, Laser processing of a SiC/Al-alloy metal matrix composite, Journal of Applied Physics 65 (1989) 5072-5077.

[4] P. Di Pietro, Y.L. Yao, A new technique to characterize and predict laser cut striations, International Journal of Machine Tools and Manufacture 35/7 (1995) 993-1002.

[5] L.A. Dobrzański, K. Gołombek, Structure and properties of the cutting tools made from cemented carbides and cermets with the TiN + mono-, gradient- or multi(Ti, Al, Si)N + TiN nanocrystalline coatings, Journal of Materials Processing Technology 164-165 (2005) 805-815.

[6] L.A. Dobrzański, M. Bonek, E. Hajduczek, A. Klimpel, A. Lisiecki, Comparison of the structures of the hot-work tool steels laser modified surface layers, Journal of Materials Processing Technology 164-165 (2005) 1014-1024.

[7] A. Dolata-Grosza, J. Śleziona, B. Formanek, Structure and properties of aluminium cast composites strengthened by dispersion phases, Journal of Materials Processing Technology 175/1-3 (2006) 192-197.

[8] J. Duan, H.C. Man, T.M. Yue, Modelling the laser fusion cutting process: II. Distribution of supersonic gas flow field inside the cut kerf, Journal of Physics D, Applied Physics 34 (2001) 2143-2150.

[9] K. Farooq, A. Kar, Removal of laser-melted material with an assist gas, Journal of Applied Physics 83/12 (1998) 74-76.

[10] A. Grabowski, M. Nowak, J. Sleziona, Optical and conductive properties of AlSi-alloy/SiCp composites: application in modelling CO_2 laser processing of composites, Optics and Lasers in Engineering 43/2 (2005) 233-246.

[11] A. Grabowski, M. Nowak, J. Sleziona, Laser cutting of an AlSi alloy/SiCp composites: theory and experiments, Journal of Achievements in Materials and Manufacturing Engineering 17 (2006) 61-64.

[12] D. Havrilla, P. Anthony, Process fundamentals of industrial laser welding and cutting, Rofin-Sinar, Inc., 1999.

[13] J.W. Kaczmar, K. Pietrzak, W. Włosinski, The production and application of metal matrix composite materials, Journal of Materials Processing Technology 106 (2000) 58-67.

[14] E. Kilickap, O. Cakir, M. Aksoy, A. Inan, Study of tool wear and surface roughness in machining of homogenised SiC-p reinforced aluminium metal matrix composite, Journal of Materials Processing Technology 164-165 (2005) 862-867.

[15] A. Manna, B. Bhattacharayya, A study on machinability of Al/SiC-MMC, Journal of Materials Processing Technology 140 (2003) 711-716.

[16] F. Müller, J. Monaghan, Non-conventional machining of particle reinforced metal matrix composite, Journal of Materials Processing Technology 118 (2001) 278-285.

[17] M. Rosso, Ceramic and metal matrix composites: route and properties, Journal of Materials Processing Technology 175/1-3 (2006) 364-375.

[18] J. Sleziona, Forming properties of the Al. ceramic particle composite produced by the casting methods, Silesian University of Technology, Gliwice, 1994 (in Polish).

[19] G. Vicanek, H. Simon, M. Urbaassek, I. Decker, Hydrodynamical instability of melt flow in laser cutting, Journal of Physics D, Applied Physics 20 (1987) 140-145.

[20] M. von Allmen, A. Blatter, Laser-Beam Interactions with Materials, Springer – Verlag, Berlin, 1995.

[21] Y. Zhou, S. Long, Y. Liu, Thermal failure mechanism and failure threshold of SiC particle reinforced metal matrix composites induced by laser beam, Mechanics of Materials 35 (2003) 1003-1020.